Real-Time Electrostatic Monitoring of Wear Debris for Wind Turbine Gearbox

Li Xin[1], *Zuo Hongfu*[1*], *Cai Jing*[1], *Sun Jianzhong*[1], *Liu Ruochen*[1,2], *Xu Yutong*[1]

1. College of Civil Aviation, Nanjing University of Aeronautics and Astronautics, Nanjing 211106, P. R. China;
2. School of Automobile and Traffic Engineering, Jiangsu University of Technology, Changzhou 213001, P. R. China

(Received 16 April 2015; revised 23 January 2016; accepted 5 February 2016)

Abstract: Engineering practice has shown that early faults of gearboxes are a leading maintenance cost driver that can easily lower the profit from a wind turbine operation. A novel oil-lubricated electrostatic monitoring of wear debris for a wind turbine gearbox is presented. The continuous wavelet transform (CWT) is used to eliminate the noises of the original electrostatic signal. The kurtosis and root mean square (RMS) values of the time domain signal are extracted as the characteristic parameters to reflect the deterioration of the gearbox. The overall tendency of electrostatic signals in accelerated life test is analyzed. In the eighth cycle, the abnormal wear in the wind turbine gearbox is detected by electrostatic monitoring. A comparison with the popular MetalScan monitoring is given to illustrate the effectiveness of the electrostatic monitoring method. The results demonstrate that the electrostatic monitoring method can detect the fault accurately.

Key words: wind turbine gearbox; oil-lubricated system; electrostatic monitoring; characteristic parameter; accelerated life test

CLC number: TH165.3 **Document code**: A **Article ID**: 1005-1120(2017)02-0195-10

0 Introduction

Due to the efficient transmission ratio and strong load capacity, gear is extensively used in aerospace, civil industry and heavy machinery with efficient transmission ratio and the strong load capacity, such as helicopters, high-speed trains and wind turbines. Condition-based maintenance (CBM) is a maintenance program that recommends maintenance actions based on the condition monitoring information with the aim to reduce system downtime, maintenance cost and improve the availability of the system[1].

Recently, in CBM program, several kinds of techniques are mainly used for full flow debris online monitoring in the oil-lubricated system of mechanical system, which are MetalScan particle monitoring sensor based on electromagnetic induction principle produced by GasTops Company in Canada, quantitative abrasive dust monitor based on induction type and oil-line electrostatic sensor based on the principle of electrostatic induction, respectively[2-4]. Among these on-line monitoring techniques, oil-line electrostatic sensor with simple and reliable structure has huge development prospects due to the high sensitivity to subtle particles and non-metallic particles. As a new on-line monitoring method, the advantage of electrostatic monitoring is that it can detect the degradation of a part much earlier and provide real-time monitoring information for maintenance decision-making compared with the traditional monitoring methods, such as vibration and temperature monitoring.

The application of gas path electrostatic monitoring technology in the aircraft engine ground simulation experiments and the integration in F-35 was firstly introduced by Powrie[4]. The mechanism of electrostatic generation was investi-

* Corresponding author, E-mail address: rms@nuaa.edu.cn.

How to cite this article: Li Xin, Zuo Hongfu, Cai Jing, et al. Real-time electrostatic monitoring of wear debris for wind turbine gearbox[J]. Trans. Nanjing Univ. Aero. Astro., 2017,34(2):195-204.
http://dx.doi.org/10.16356/j.1005-1120.2017.02.195

gated on a pin-on-disc wear test rig and the oil-lubricated point contact wear test was conducted by Morris and Harvey et al[5-6]. Under the unlubricated condition, both acoustic emission and electrostatic monitoring techniques were respectively adopted to carry out the online monitoring of early stage of the severe wear of bearing steel by Sun and Wood et al[7]. The root mean square (RMS) values of these monitoring methods can reflect the three stages of abrasion, running-in, delamination and oxidation. Harvey et al. considered the combination of the wear-site sensor (WSS), vibrating sensor and temperature sensor to monitor the early failure of wear area in a conical roller bearing[8]. However, the existing literature is only limited to the applications, and the principles of the electrostatic mechanism is quite few.

Wen et al. have investigated the electrostatic monitoring since 2007[9-11], and the electrostatic monitoring sensors used in gas path of the aeroengine have been designed, also the sensitivity of the sensor has been analyzed using finite element method. Meanwhile, the aeroengine gas path simulation test platform has been established and a preliminary test has been completed. The leakage fault of the lubricating oil was detected in a small turbojet engine[12-13]. Subsequently, the research of electrostatic oil-line and wear-site sensors was tentatively carried out[14], the preliminary design of the oil-line electrostatic sensor was finished, and the verification test of which was conducted on a turbojet engine[15] and ABLT-1A type bearings fatigue life test rig[16].

It should be noted, however, the existing research of lubricating oil-line electrostatic monitoring is mainly concentrated in pin-on-disc wear test and rolling bearing performance degradation test, which are relatively simple systems in laboratory. The research of high speed, overloaded and complex oil-lubricated electrostatic monitoring of gearbox has not started yet. In this paper, a real-time electrostatic monitoring of debris in full flow oil-lubricated system of gearbox is carried out in a new type of wind turbine gearbox test rig. The electrostatic signals are obtained.

1 Experimental Scheme of Electrostatic Monitoring for a Wind Turbine Gearbox

1.1 Experimental set-up and data collection

The accelerated life test (ALT) is designed to validate the performance of the gearbox in operating range and check if the gearbox can function well under different load conditions. Fig. 1 illustrates the principle of lubricating oil-line abrasive electrostatic monitoring in the wind turbine gearbox. The abrasive particles in the gearbox lubricating oil-line are charged by the energy produced by the friction and wear. The electric charges will be generated on the rapiers when the charged particles go through the induction area of the oil-line electrostatic sensors. The corresponding signals are collected via the signal acquisition device, and the signal disposal and fault characteristic extracting are completed by the signal acquisition and processing system.

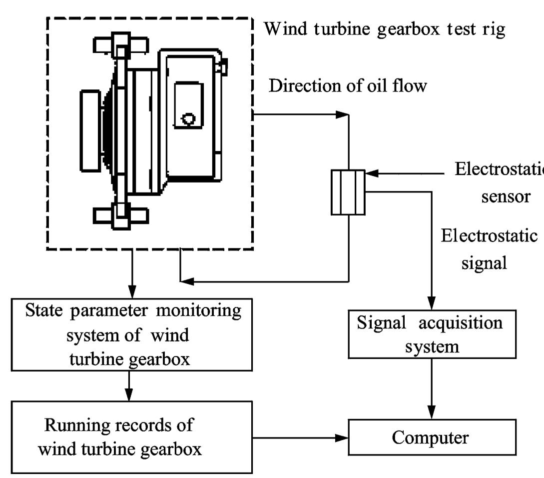

Fig. 1 Principle of electrostatic monitoring in wind turbine gearbox

A new type of wind turbine gearbox is used for this experiment, which is a typical two-stage planetary and two levels of parallel structure. Table 1 provides the specifications of the wind turbine gearbox.

Table 1　Wind turbine gearbox information

Parameter	Specification
Rated power/kW	3 499.5
Transmission ratio	117.50
Lubricating oil brand	Castrol Optimol Optigear X320
Lubricating oil volume/L	425
Oil flow speed/(L · min^{-1})	225
Tube inner diameter/mm	51
Filter accuracy/μm	50
Drive motor power/kW	8 000
Data acquisition card	NI-WLS9234
Charge amplifier	YE5854A
Sampling frequency/kHz	10

Gearbox is run under a certain speed which is driven by a drive motor, and the load can be changed by adjusting the torquemeter. The gearbox is installed on the test rig, and electrostatic sensor is installed in the oil outlet. MetalScan particles monitor (Main function is counting particles) is installed in the downstream of the electrostatic sensor, signal acquisition system in the experiment control office which is connected to the electrostatic sensor by a shielding data line. Fig. 2 illustrates the integrated testing plan.

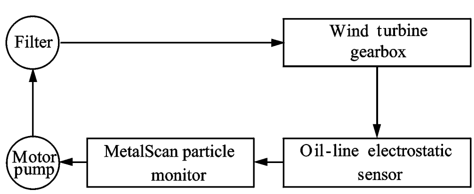

Fig. 2　Experimental scheme for lubricating oil electrostatic monitoring in wind turbine gearbox

1.2　Electrostatic sensor and installation

There are several forms of electrostatic sensors, such as annular and virgate. Annular electrostatic sensor is selected in this experiment. Fig. 3 provides the image of the annular oil-line electrostatic sensor. Red copper with high conductivity is chosen to be the material of the induction rapiers, the radial thickness of which is negligible. The rapiers are implanted into the tube wall made of teflon and are sealed by epoxy resin with the minimum conductivity. Shell of the sensor is made of stainless steel with the aim of electromagnetic shielding.

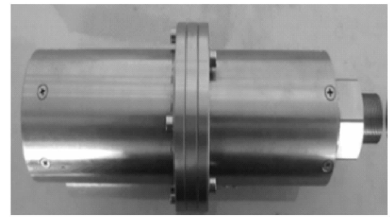

Fig. 3　Structure of annular oil-line electrostatic sensor

Fig. 4 shows the induction principle of annular electrostatic sensor. When charged particles go through the measurement space of electrostatic sensor, electric charge will be induced on rapiers correspondingly, which will be transformed to output signals can be measured by signal processing circuit.

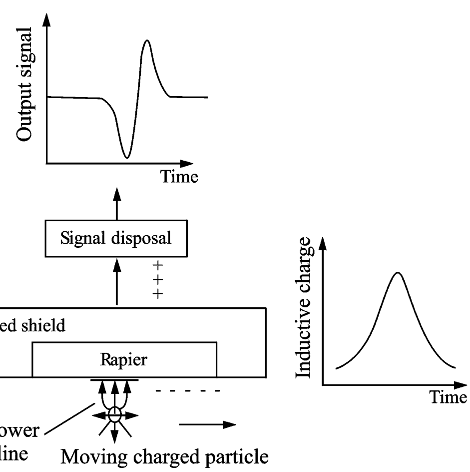

Fig. 4　Sensing principle of electrostatic sensor

The output voltage of electrostatic sensor at time t [17]

$$u_0 = \frac{R_i rqv}{2R_f \pi} \int_0^{\pi} \left\{ \frac{r - x\cos\phi}{[(vt + L)^2 + F^2(x, \phi)]^{\frac{3}{2}}} - \frac{r - x\cos\phi}{[(vt - L)^2 + F^2(x, \phi)]^{\frac{3}{2}}} \right\} d\phi \tag{1}$$

where u_0 is the output voltage, R_f the feedback resistance, R_i the equivalent resistance, r the radius of the rapier, q the charge of abrasive particle, v the kinematic velocity, L the axial length of the rapier, x the x-axis value of the projected length of the particle, ϕ the angle between a point that on the circumference and x-axis, and $F(x, \phi)$ the distance between the projected point and the point on the circumference.

The actual installation situation of annular oil-line electrostatic sensor in the gearbox test rig is shown in Fig. 5.

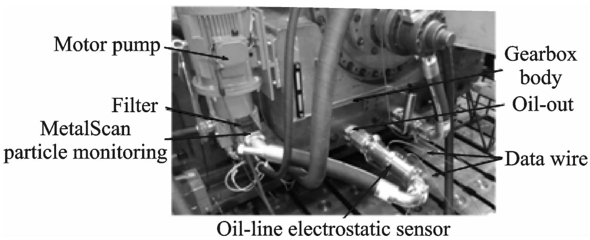

Fig. 5 Installation location map of oil-line electrostatic sensor

2 Electrostatic Signal Processing

The time-domain analysis methods are employed to process the electrostatic signal. The overall process of the original electrostatic data for the wind turbine gearbox is illustrated schematically in Fig. 6.

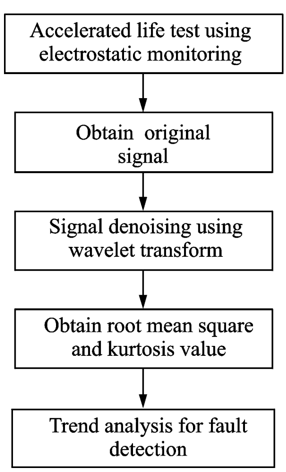

Fig. 6 Flowchart of fault detection process

2.1 Original electrostatic signal

In the electrostatic monitoring system of the wind turbine gearbox, the acquisition of electrostatic signals starts at the beginning of each test cycle and ends at the end of the cycle when the speed drops to 0. As illustrated in Section 1.2, the original signals collected by oil-line electrostatic sensors are voltage signals. Fig. 7 presents the original electrostatic signals of the normal steady state under 100% rated torque. Fig. 8 shows the original electrostatic signals when charged wear particles go through.

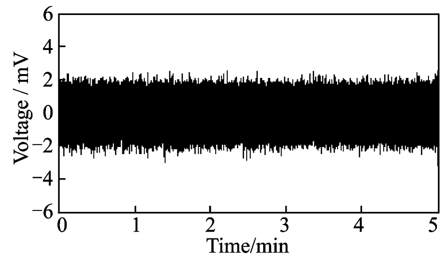

Fig. 7 Original electrostatic signal under normal circumstances

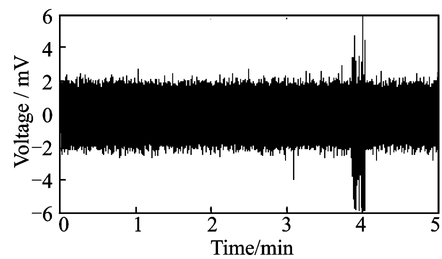

Fig. 8 Original electrostatic signal as charged particles passing

As shown in Fig. 7, the electrostatic signals are relatively smooth and steady under the stable conditions, while the voltage values fluctuate in a certain scope. When there is severe or abnormal wear in the gearbox, as shown in Fig. 8, at the 4th minute, electrostatic signal outputs are beyond the normal range and some mutation pulses appear due to the increase of the wear particles.

2.2 Feature extraction using wavelet method

We choose wavelet transform to eliminate the noises of the original electrostatic signal. Wavelet transform is a powerful method for studying how the frequency content changes with time and consequently is able to detect and localize short-duration phenomena, and it has been used in the fault diagnosis of rotating machinery extensively in recent years[18-19].

The continuous wavelet transform (CWT) uses a series of oscillating functions with different frequencies as window functions to scan and translate the original signal. The mother wavelet is given by

$$\varphi_{\alpha,\beta}(t)=\alpha^{-1/2}\int_{-\infty}^{+\infty}\varphi\left(\frac{t-\beta}{\alpha}\right)\mathrm{d}t \tag{2}$$

where $\varphi_{\alpha,\beta}(t)$ is the window function, α the dilation parameter, and β the translation parameter.

Suppose that all the signals satisfy the condition

$$\int_{-\infty}^{+\infty} |V(t)|^2 \mathrm{d}t < \infty \tag{3}$$

which implies that decays to zero.

Thus, the wavelet transform of a time-domain signal V_t is given by

$$\mathrm{CWT}(\alpha,\beta) = \alpha^{-1/2}\int_{-\infty}^{+\infty} V_t \varphi^* \left(\frac{t-\beta}{\alpha}\right) \mathrm{d}t \tag{4}$$

where $\varphi^*(t)$ is the complex conjugate of the analyzing wavelet $\varphi(t)$.

The conventional feature extraction methods in time-domain of electrostatic signal and vibration monitoring are similar and the main indicators include crest value, peak-peak value, kurtosis, root mean square (RMS) value, impulse factor, etc. More details can be found in Ref. [20]. These parameters can describe the change process from normal wear to abnormal wear condition. Table 2 shows the main parameters in the time domain characteristic extraction.

Table 2 Extraction parameters of time-domain feature for electrostatic signal

Feature	Equation	Feature	Equation
RMS	$x_{\mathrm{rms}} = \sqrt{\sum_{n=1}^{N} (x(n))^2 / N}$	Kurtosis	$x_{\mathrm{kur}} = \sum_{n=1}^{N} (x(n) - x_m)^4 / ((N-1) x_{\mathrm{std}}^4)$
Standard deviation	$x_{\mathrm{std}} = \sqrt{\sum_{n=1}^{N} (x(n) - x_m)^2 / (N-1)}$	Crest factor	$\mathrm{CF} = x_p / x_{\mathrm{rms}}$
Peak-Peak	$x_{\mathrm{p-p}} = \max(x_n) - \min(x_n)$	Impulse factor	$\mathrm{IF} = x_p \Big/ (\sum_{n=1}^{N} \lvert x(n) \rvert / N)$
Skewness	$x_{\mathrm{ske}} = \sum_{n=1}^{N} (x(n) - x_m)^3 / ((N-1) x_{\mathrm{std}}^3)$	Clearance factor	$\mathrm{CLF} = x_p \Big/ (\sum_{n=1}^{N} \sqrt{\lvert x(n) \rvert} / N)^2$

As shown in Table 2, N represents the total number of signal values, $x(n)$ the electrostatic signal value; $\max x_n$ and $\min x_n$ are the maximum and the minimum voltage signal values in sampling points n, respectively.

RMS is commonly used as the electrostatic signal characteristic parameters, representing the effective value of induction charge responding in the sensor when electric charges pass through the sensing area in a certain time interval[7,14]. As the wear degree aggravating, the number of charged wear particles is growing. If the number of induction charges passing the sensing areas increases per unit time (1 s), the output signal amplitude and the RMS values of the sensor will also rise. Simultaneously, as a dimensional parameter, RMS is more sensitive to the variation of signal amplitude and energy. Therefore, it is selected as the indicator to process the electrostatic signal in this paper.

Generally, the vibration signal of the mechanical system is periodic, and it can be approximated by the sum of several sinusoidal signals. While the electrostatic signal that obtained in this experiment is nonperiodic, i. e. the signal is random, it is more likely the exponential decay signal. The exponential decay signal can be treated as impulse signal, and the kurtosis is very sensitive to the impulse signal[21-22]. Therefore, it is desirable to consider the kurtosis to extract the feature of the electrostatic signal. Thus, in this paper, two kinds of the time-domain characteristic parameters, namely RMS and kurtosis are selected to describe the wear conditions of the wind turbine gearbox.

3 Results and Discussion

3.1 Accelerated Life Electrostatic Monitoring Test

The performance of the gearbox under rated load/overload/extreme load conditions is validated by ramp-up test, and the speeds of the high-speed shaft and low-speed shaft are constant. Each test phase is divided into 16 short stages, each of which lasts 571 min. The test schedule for ALT is introduced in Table 3.

Table 3 Testing schedule for accelerated life test

Load stage/ %	Low speed shaft speed/ (r • min^{-1})	Low speed shaft torque/ (kN • m)	High speed shaft speed/ (r • min^{-1})	High speed shaft torque/ (N • m)	Time/ min
18	14.78	414	1 736.6	3 523.5	0.5
29	14.78	667	1 736.6	5 676.8	0.5
38	14.78	874	1 736.6	7 438.5	0.5
46	14.78	1 058	1 736.6	9 004.5	0.5
53	14.78	1 219	1 736.6	10 374.8	1.5
60	14.78	1 380	1 736.6	11 745.0	0.5
70	14.78	1 610	1 736.6	13 702.5	0.5
80	14.78	1 840	1 736.6	15 660.0	0.5
90	14.78	2 070	1 736.6	17 617.5	0.5
100	14.78	2 300	1 736.6	19 575.0	80
125	14.78	2 875	1 736.6	24 468.8	80
150	14.78	3 450	1 736.6	29 362.5	360
165	14.78	3 795	1 736.6	32 298.8	25
175	14.78	4 025	1 736.6	34 256.3	15
185	14.78	4 255	1 736.6	36 213.8	5
200	14.78	4 600	1 736.6	39 150.1	0.5
Accumulated test time/min					571

As shown in Table 3, the total test time under the condition of 18%—90% and 165%—200% rated torque is relatively short. For convenience, each cycle is divided into 5 stages, recorded as before 100%, 100%(rated load), 125% (overload), 150%(overload) and after 150% (extreme load).

In a single test cycle under normal condition, for example, using the signal processing method in Section 2, the trend of the RMS values in a whole test cycle is described in Fig. 9. The kurtosis of electrostatic signal in a single cycle is shown in Fig. 10.

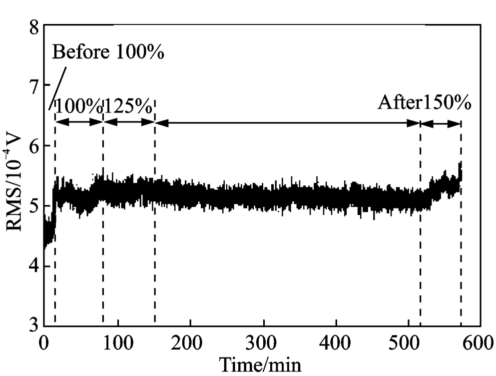

Fig. 9 RMS values of electrostatic signal in a single cycle of accelerated life test

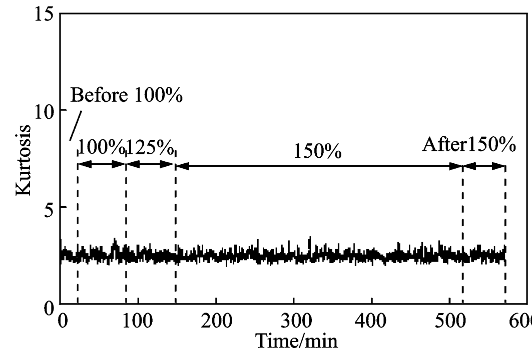

Fig. 10 Kurtosis of electrostatic signal in a single cycle of accelerated life test

The effect of rotation speed variation on the gearbox static level need not to be considered because each stage of the accelerated life test is under the same speed. In Fig. 9, 0—9.5 min represents the stage of before 100% load test, 9.5—89.5 min the stage of 100% rated load test; 89.5—169.5 min and 169.5—525.5 min represent the stage of 125% and 125% overload test, respectively, 525.5—571 min represents the stage of after 150% extreme load test. In before 100% stage, lubricating oil electrostatic monitoring signal shows a continuous rise with the increasing torque. This stage reflects the production of small particles in the lubricated system in the continuous load test stage, although the duration is short. In 100% stage, electrostatic monitoring value is high at the beginning, then declines slightly, eventually slowly increases and stabilizes at a certain level. In 125% overload test stage, the value tends to be stable, but higher than 100% test stage. The gearbox condition has not changed within the 360 min in the longest 150% overload test stage, remaining under stable wear state, as well as the lubricating oil electrostatic monitoring value. In after 150% extreme load test stage, electrostatic monitoring signal also shows a trend of continuous rising with the increase of torque, which is consistent with the before 100% stage, but the overall electrostatic level is much higher than the before 100% stage.

We can further find that the torques are much higher than the rated load in the extreme load test stage, leading to the gears and bearings under overload operation. Although the duration is short, the electrostatic monitoring signal shows that electrostatic charges generated from the gearbox internal wear increase, leading to the increasing inductive charges sensed by the electrostatic sensor in the lubricated system. This is in accordance with the theoretical analysis of the relationship between the charges of particles in friction pairs and the loads under the condition of oil lubrication[6], thus it demonstrates the feasibility of the application of the oil-line electrostatic sensors for the on-line monitoring for the wear conditions of wind turbine gearbox.

While in Fig. 10, the kurtosis of electrostatic signal in a single cycle indicates that the kurtosis is relatively stable, and it is not sensitive to the load variations. The stationary kurtosis shows that the gearbox is run in the normal condition, and the amplitude of kurtosis will increase when more debris passed by in the oil system.

3.2 Overall trend analysis

In the accelerated life test, data of 9 test cycles in electrostatic monitoring are obtained, which is processed using the method in Section 2. We obtain the change trend of static values along with the test cycles on the large time scale, which are shown in Figs. 11,12, respectively.

As shown in Fig. 11, the RMS values of the electrostatic signal fluctuate at each cycle of ALT, which is similar to the single test cycle analysized in Section 3. 1. The main reason for which is that the electrostatic signals in the lubricated system will be affected by the torque in each cycle. From Cycle 1 to 7, electrostatic RMS value in each cycle tends to be stable and is similar to that in other cycles. Only a few larger values appear in Cycles 2, 3 and 5, indicating some charged particles exist in the oil. Suppose that the charge of the debris is saturated, so the greater the carrying capacity is, the greater the equivalent diameter of particles is[23]. About the last 15 min in the 8th cycle (late stage after 150%), the RMS values are significantly higher than the overall level of the cycles before, with a large number of abnormal values appearing sharply, which represents that a large number of large diameter particles pass the electrostatic sensor in the lubricated system in this period. It is also proved by the monitoring data of MetalScan monitor installed downstreams. After the 8th cycle, stop the test to examine and continue testing after debugging. The RMS value recovers to normal level in the 9th test cycle.

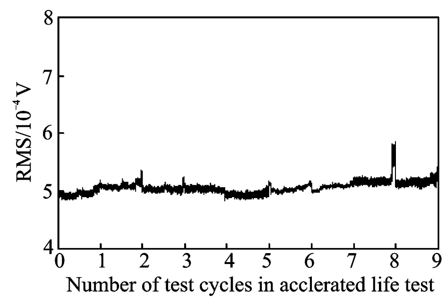

Fig. 11 RMS trend in 1—9 test cycles

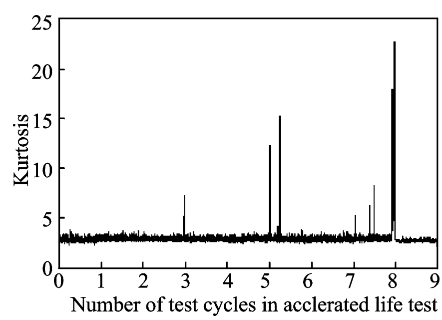

Fig. 12 Kurtosis trend in 1—9 test cycles

The overall trend of kurtosis in Fig. 12 is similar to the results that obtained by the RMS values. The amplitude of kurtosis is stable except in Cycles 3, 5 and 7, but the impulses are not too many. While at the end of the 8th cycle, the impulses increase significantly, which means the gearbox experience severe deterioration. The wind turbine gearbox should be stopped immediately and full system inspection should be performed.

3.3 Comparison of MetalScan analysis

The common methods of gearbox condition

monitoring contain oil particle counting[24] and oil spectrometric analysis[25]. To test and verify the effectiveness of oil-line electrostatic monitoring, the data that obtained by MetalScan monitoring is used to analyze and compare with electrostatic monitoring data. The MetalScan, with 2 inches for inner diameter, can identify the larger particles that the equivalent diameter is larger than 1mm. In the process of test, record the total number of particles in 5 stages of each test cycle, respectively, and MetalScan monitoring data of all nine cycles are provided in Table 4.

Table 4 MetalScan monitoring data

Load	Cycle 1	Cycle 2	Cycle 3	Cycle 4	Cycle 5	Cycle 6	Cycle 7	Cycle 8	Cycle 9
Before 100%	3	1	0	1	3	6	2	11	3
100%	6	8	3	4	1	2	0	3	6
125%	12	4	7	2	0	4	0	7	5
150%	3	9	12	11	25	11	3	4	6
After 150%	15	8	22	3	9	5	4	584	19

As shown in Table 4, the number of particles is small from Cycle 1 to 7, which shows that gearbox runs stably, while it increases suddenly to 584 in the after 150% stage of the 8th cycle, representing abnormal wear appears and decreases to normal level in the 9th cycle. This is identical with the results of oil-line static analyzed in Section 3.2, verifying the validity of the electrostatic monitoring. However, the electrostatic sensor has more advantage in sensing the concentration of molecules, which can reflect the change of working condition of gearbox, while MetalScan sensor can just sense and count large particles.

According to the gearbox fault detection report, the causes of the abnormal wear in after 150% stage of the 8th cycle in electrostatic monitoring and MetalScan monitor are that the membrane coupling of high-speed output shaft produces fatigue cracks, leading to the high-speed output shaft prejudicially revolve and the number of particles add due to the corrosive pitting of the gear tooth roots of the high-speed shaft. The effectiveness of oil electrostatic monitoring is validated further. Fig. 13 shows the results of fatigue cracks and tooth root pitting.


(a) Membrane fatigue crack


(b) Tooth root pitting

Fig. 13 Schematic diagram of membrane fatigue crack and tooth root pitting

4 Conclusions

The oil-line electrostatic sensor installed in the wind turbine gearbox test rig is used for online monitoring, obtaining the characteristics of electrostatic signals in the lubricated system through the gearbox vibration routine test and accelerated life test. And the conclusions are as follows:

(1) The annular oil electrostatic sensor has been installed in the wind turbine gearbox test rig for the first time, and the on-line monitoring of lubricated system has been carried out, which verifies the on-line electrostatic monitoring technology is feasible for application in the wind turbine gearbox.

(2) The continuous wavelet transform method is used to eliminate the noises of the original electrostatic signal. Two indicators, namely kurtosis and RMS values of the time-domain signal are extracted as the characteristic parameters to reflect the deterioration process of the gearbox.

(3) Electrostatic monitoring in the accelerated life test shows the formation of fine particles in the lubricating oil under rated load/overload/extreme load conditions. The RMS values change synchronously along with the load variations. The kurtosis is relatively stable and not sensitive to the load variations.

(4) A large number of large amplitude anomaly points of the RMS values and kurtosis appears in the after 150% stage of the 8th cycle during the test, and membrane fatigue cracks and tooth root pitting are found in the gearbox fault inspection, which demonstrate the effectiveness of the oil-line electrostatic monitoring technique.

(5) The comparison of MetalScan monitor data further shows the efficiency of the on-line monitoring method. Based on the promising results we obtained, the life prediction and optimal maintenance policy can be studied, which can be a suitable topic for the future research.

Acknowledgements

This paper was co-supported by the National Natural Science Foundation of China (Nos. 61403198, BK20140827 and U1233114), the Funding of Jiangsu Innovation Program for Graduate Education (No. KYLX15_0313), the Fundamental Research Funds for the Central Universities (No. NS2015072). Also, the support provided by China Scholarship Council (No. 201606830028) during a visit of Li Xin at the University of Toronto is acknowledged and appreciated.

References:

[1] AHMAD R, KAMARUDDIN S. An overview of time-based and condition-based maintenance in industrial application[J]. Computers & Industrial Engineering, 2012, 63(1): 135-149.

[2] MILLER J L, KITALJEVICH D. In-line oil debris monitor for aircraft engine condition assessment [C]// IEEE Aerospace Conference Proceedings. Big Sky, Montana, USA. Piscataway: IEEE, 2000(6): 49-56.

[3] BYINGTON C S, SCHALCOSKY D C. Advances in real time oil analysis [J]. Practicing Oil Analysis Magazine, 2000, 11(2): 28-34.

[4] POWRIE H. Use of electrostatic technology for aero engine oil system monitoring[C]//IEEE Aerospace Conference Proceedings. [S. l.]: IEEE, 2000: 57-71.

[5] MORRIS S, WOOD R, HARVEY T J, et al. Use of electrostatic charge monitoring for early detection of adhesive wear in oil lubricated contacts [J]. Journal of Tribology Transactions of the ASME, 2002, 124(2): 288-296.

[6] HARVEY T J, MORRIS S, WANG L, et al. Real-time monitoring of wear debris using electrostatic sensing techniques [J]. Proc IMechE Part J: Journal of Engineering Tribology, 2007, 221(1): 27-40.

[7] SUN J, WOOD R J K, WANG L, et al. Wear monitoring of bearing steel using electrostatic and acoustic emission techniques [J]. Wear, 2005, 259(7): 1482-1489.

[8] HARVEY T J, WOOD R J K, POWRIE H E G. Electrostatic wear monitoring of rolling element bearings [J]. Wear, 2007, 263(7): 1492-1501.

[9] WEN Zhenhua, ZUO Hongfu, LI Yaohua. Gas path debris electrostatic monitoring technology and experiment [J]. Journal of Aerospace Power, 2008, 23(12): 2321-2326. (in Chinese)

[10] LI Yaohua, ZUO Hongfu, WEN Zhenhua, et al. Simulated experiment of aircraft engine gas path debris monitoring technology [J]. Acta Aeronoutica et Astronautica Sinica, 2009, 30(4): 604-608. (in Chinese)

[11] WEN Zhenhua, ZUO Hongfu, LI Yaohua, et al. New method for aero engine gas path monitoring [J]. Journal of Nanjing University of Aeronautics & Astronautics, 2009, 21(2): 248-252. (in Chinese)

[12] LIU Pengpeng, ZUO Hongfu, FU Yu, et al. Exhaust gas electrostatic monitoring and gas path fault feature for turbojet engine [J]. Journal of Aerospace Power, 2013, 28(2): 473-480. (in Chinese)

[13] LIU P P, ZUO H F, SUN J Z. The electrostatic

sensor applied to the online monitoring experiments of combustor carbon deposition fault in aero-engine [J]. IEEE Sensors Journal, 2014, 14(3): 686-694.

[14] CHEN Zhixiong, ZUO Hongfu, ZHAN Zhijuan, et al. Study of oil system oil-line debris electrostatic monitoring technology [J]. Acta Aeronautica et Astronautica Sinica, 2012, 33(3): 446-452. (in Chinese)

[15] FU Y, ZUO H F, LIU P P, et al. Gas path electrostatic sensor monitoring and comparison experiment on turbojet engine[J]. Transactions of Nanjing University of Aeronautics and Astronautics, 2013, 30 (4):361-365.

[16] LIU Ruochen, ZUO Hongfu. Research on electrostatic monitoring method of rolling bearings with injected fault under variable operating conditions [J]. Chinese Journal of Scientific Instrument, 2014, 35 (10): 2348-2355. (in Chinese)

[17] HUANG Wenjie, ZUO Hongfu. Research on electrostatic sensing for in-line abrasive monitoring in full flow oil system [J]. Acta Aeronoutica et Astronautica Sinica, 2013, 34(8): 1786-1794. (in Chinese)

[18] CHEN J, LI Z, PAN J, et al. Wavelet transform based on inner product in fault diagnosis of rotating machinery: A review[J]. Mechanical Systems and Signal Processing, 2016, 70: 1-35.

[19] ESPOSITO A, RUSSO L, KANDLER C, et al. High fuel utilization in solid oxide fuel cells: Experimental characterization and data analysis with continuous wavelet transform [J]. Journal of Power Sources, 2016, 317: 159-168.

[20] ZHANG Ying, ZUO Hongfu, CHEN Zhixiong, et al. Electrostatic monitoring of oil lubricated sliding bearing steel with point contacts for detection of initial stage of scuffing [J]. Tribology, 2012, 32(5): 507-515. (in Chinese)

[21] WANG Y, XIANG J, MARKERT R, et al. Spectral kurtosis for fault detection, diagnosis and prognostics of rotating machines: A review with applications[J]. Mechanical Systems and Signal Processing,2016, 66/67: 679-698.

[22] TIAN J, MORILLO C, AZARIAN M H, et al. Motor bearing fault detection using spectral kurtosis-based feature extraction coupled with K-nearest neighbor distance analysis[J]. IEEE Transactions on Industrial Electronics, 2016, 63(3): 1793-1803.

[23] BOUSLIMI Y, FOFANA I, HEMMATJOU H, et al. Static electrification assessment of transformer oils in the spinning disc system [C]//High Voltage Engineering and Application (ICHVE), International Conference on. [S. l.]: IEEE, 2010: 337-340.

[24] LOUTAS T H, ROULIAS D, PAULY E, et al. The combined use of vibration, acoustic emission and oil debris on-line monitoring towards a more effective condition monitoring of rotating machinery[J]. Mechanical systems and signal processing, 2011, 25 (4): 1339-1352.

[25] SHENG S. Monitoring of wind turbine gearbox condition through oil and wear debris analysis: A full-scale testing perspective[J]. Tribology Transactions, 2016, 59(1): 149-162.

Mr. **Li Xin** received his B. S. degree in College of Mechanical and Electrical Engineering from Zhengzhou Institute of Aeronautical Industry Management in 2012. He is now a Ph. D. candidate at Nanjing University of Aeronautics and Astronautics (NUAA). His research interests are maintenance, system engineering and prognostic and health management (PHM). He is a visiting Ph. D. student in the condition-based maintenance lab at the University of Toronto from October 2016 to October 2017.

Prof. **Zuo Hongfu** received his Ph. D. degree from China University of Mining and Technology in 1989. Now he is a professor and doctoral supervisor at Nanjing University of Aeronautics and Astronautics (NUAA). His research interests include maintenance, system engineering and prognostic and health management (PHM).

Dr. **Cai Jing** received his Ph. D. degree from Nanjing University of Aeronautics and Astronautics (NUAA) in 2007. Now he works as a teacher at Nanjing University of Aeronautics and Astronautics. His research interests include reliability statistics, maintenance theory and prognostic and health management (PHM).

Dr. **Sun Jianzhong** received his Ph. D. degree from Nanjing University of Aeronautics and Astronautics (NUAA) in 2012. Now he is an associate professor at NUAA. His research interests include aircraft prognostic and health management (PHM) and maintenance engineering.

Dr. **Liu Ruochen** received his B. S. and Ph. D. degrees from Nanjing University of Aeronautics and Astronautics (NUAA) in 2011 and 2016, respectively. He is currently a lecturer with School of Automobile and Traffic Engineering, Jiangsu University of Technology. His main research interests include advanced sensors, theoretical model and experiment, state monitoring, and fault detection.

Mr. **Xu Yutong** received his B. S. degree from Nanjing University of Aeronautics and Astronautics (NUAA) in 2015. He is now a postgraduate student at NUAA. His main research interests include reliability statistics, maintenance theory and prognostic and health management (PHM).

(Executive Editor: Xu Chengting)